Sliding Mode Controls of Active and Reactive Power of a DFIG with MPPT for Variable Speed Wind Energy Conversion

2 authors:

Youcef Bekakra
El-Oued University
17 PUBLICATIONS **73** CITATIONS

SEE PROFILE

Djilani ben attous
El-Oued University
95 PUBLICATIONS **195** CITATIONS

SEE PROFILE

Sliding Mode Controls of Active and Reactive Power of a DFIG with MPPT for Variable Speed Wind Energy Conversion

Youcef Bekakra and Djilani Ben Attous

Department of Electrical Engineering, El-Oued University Center, Algeria.

Abstract: This paper presents the study of a variable speed wind energy conversion system based on a Doubly Fed Induction Generator (DFIG) based on a sliding mode control applied to achieve control of active and reactive powers exchanged between the stator of the DFIG and the grid to ensure a Maximum Power Point Tracking (MPPT) of a wind energy conversion system. The proposed control algorithm is applied to a DFIG whose stator is directly connected to the grid and the rotor is connected to the PWM converter. To extract a maximum of power, the rotor side converter is controlled by using a stator flux-oriented strategy. The created decoupling control between active and reactive stator power allows keeping the power factor close to unity. Simulation results show that the wind turbine can operate at its optimum energy for a wide range of wind speed.

Key words: Doubly Fed Induction Generator, Wind Energy, Wind Turbine, Sliding Mode Control, Maximum Power Point Tracking (MPPT).

INTRODUCTION

Recently, the doubly fed induction generator (DFIG) is becoming the main configuration of wind power generation because of its unique advantages. Vector control technology is used to control the generator, and the rotor of DFIG is connected to an AC excitation of which the frequency, phase, and magnitude can be adjusted. Therefore, constant operating frequency can be achieved at variable wind speeds (Guo-qing, W.U., 2010).

A doubly fed induction generator is most commonly used in wind power generation. It is a wound rotor induction machine with slip rings attached at the rotor and fed by power converter. With DFIG, generation can be accomplished in variable speed ranging from sub-synchronous speed to super-synchronous speed (Jeong-Ik Jang, 2006).

The variable speed constant frequency (VSCF) wind power generation is mainly based on the research of optimal power-speed curve, namely the most mechanical power of turbine can be achieved by regulating the speed of generator, where the wind speed may be detected or not (Guo-qing, W.U., 2010).

Through studying the characteristics of wind turbine, the paper proposed the maximum power point tracking (MPPT) control method. Firstly, according to the DFIG character, the paper adopts the vector transformation control method of stator oriented magnetic field to realize the decoupling control for the active power and reactive power using sliding mode control (SMC).

Sliding mode theory, stemmed from the variable structure control family, has been used for the induction motor drive for a long time. It has for long been known for its capabilities in accounting for modelling imprecision and bounded disturbances. It achieves robust control by adding a discontinuous control signal across the sliding surface, satisfying the sliding condition. Nevertheless, this type of control has an essential drawback, which is the chattering phenomenon caused from the discontinuous control action. To alleviate the chattering phenomenon, the idea of boundary layer is used to improve it. It is called a modified controller. In this method, the control action was smoothed such that the chattering phenomenon can be decreased (Hazzab, A., 2005).

In this paper, we apply the SMC method to the wind energy conversion systems to design a novel MPPT control algorithm.

2. Model of Turbine:

The wind turbine input power usually is (Xuemei Zheng, 2009):

$$P_v = \frac{1}{2}\rho S_w v^3 \tag{1}$$

where ρ is air density; S_w is wind turbine blades swept area in the wind; v is wind speed.
The output mechanical power of wind turbine is:

Corresponding Author: Youcef Bekakra, Department of Electrical Engineering, El-Oued University Center, Algeria.
E-mail: youcef1984@gmail.com, dbenattous@yahoo.com

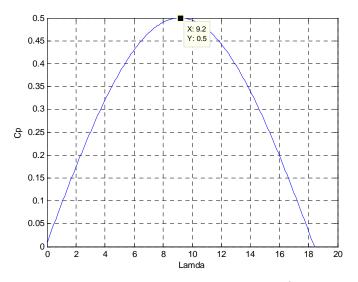$$P_m = C_p P_v = \frac{1}{2} C_p \rho S_w v^3 \qquad (2)$$

where C_p represents the wind turbine power conversion efficiency. It is a function of the tip speed ratio λ and the blade pitch angle β in a pitch-controlled wind turbine. λ is defined as the ratio of the tip speed of the turbine blades to wind speed:

$$\lambda = \frac{R\,\Omega_t}{v} \qquad (3)$$

Where R is blade radius. Ω is angular speed of the turbine.
C_p can be described as (Salma El-Aimani, 2004):

$$C_p(\beta, \lambda) = (0.5 - 0.0167*(\beta - 2)).sin(\pi.(\lambda + 0.1)/(18.5 - 0.3.(\beta - 2))) - 0.00184.(\lambda - 3).(\beta - 2) \qquad (4)$$

A figure showing the relation between C_p and λ is shown in figure 1. The maximum value of C_p ($C_{p\_max} = 0.5$) is achieved for $\beta = 2$ degree and for $\lambda_{opt} = 9.2$.

Fig. 1: Aerodynamic power coefficient variation C_p against tip speed ratio λ .

3. Maximum Power Point Tracking (MPPT):

Maximum power variation with rotation speed Ω of DFIG is predefined for each wind turbine. So for MPPT, the control system should follow the tracking characteristic curve (TCC) of the wind turbine (Ali M. Eltamaly, 2010). Each wind turbine has TCC similar to the one shown in figure 2. The actual wind turbine, Ω is measured and the corresponding mechanical power of the TCC is used as the reference power for the power control loop (Ali M. Eltamaly, 2010).

In order to make full use of wind energy, in low wind speed β should be equal to 2°. Figure 2 illustrates the wind turbine power curve when β is equal to 2°.

To extract the maximum power generated, we must fix the advance report λ_{opt} is the maximum power coefficient C_{p_max} , the measurement of wind speed is difficult, an estimate of its value can be obtained :

$$v_{est} = \frac{R.\Omega_t}{\lambda_{otim}} \qquad (5)$$

The electromagnetic power must be set to the following value:

$$P_{em\_ref} = \frac{1}{2} C_{p\_max} \cdot \rho \cdot S_w \cdot v_{est}^3 / \Omega_t \tag{6}$$

From the figure 2 we can see there is one specific angular frequency at which the output power of wind turbine is maximum occurs at the point where C_p is maximized.. Connected all the maximum power point of each power curve, the optimal power curve (P_{optim} curve) is gotten.
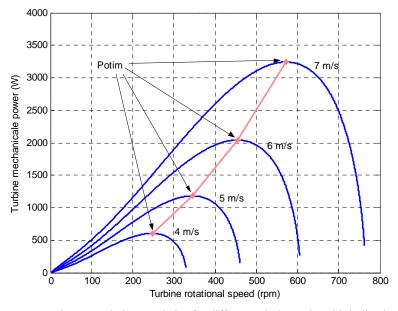

Fig. 2: Turbine powers various speed characteristics for different wind speeds, with indication of the maximum power tracking curve.

4. Modelling of the DFIG:

The general electrical state model of the induction machine obtained using Park transformation is given by the following equations (Utkin, V.I., 1993):

Stator and rotor voltages:

$$\begin{cases} V_{sd} = R_s i_{sd} + \dfrac{d}{dt}\phi_{sd} - \omega_s \cdot \phi_{sq} \\[2mm] V_{sq} = R_s i_{sq} + \dfrac{d}{dt}\phi_{sq} + \omega_s \cdot \phi_{sd} \\[2mm] V_{rd} = R_r i_{rd} + \dfrac{d}{dt}\phi_{rd} - (\omega_s - \omega)\cdot\phi_{rq} \\[2mm] V_{rq} = R_r i_{rq} + \dfrac{d}{dt}\phi_{rq} + (\omega_s - \omega)\cdot\phi_{rd} \end{cases} \tag{7}$$

Stator and rotor fluxes:

$$\begin{cases} \phi_{sd} = L_s i_{sd} + M i_{rd} \\[2mm] \phi_{sq} = L_s i_{sq} + M i_{rq} \\[2mm] \phi_{rd} = L_r i_{rd} + M i_{sd} \\[2mm] \phi_{rq} = L_r i_{rq} + M i_{sq} \end{cases} \tag{8}$$

The electromagnetic torque is done as:

$$C_e = pM (i_{rd} i_{sq} - i_{rq} i_{sd}) \tag{9}$$

and its associated motion equation is:

$$C_e - C_r = J\frac{d\Omega}{dt} \tag{10}$$

The state variable vector is then :

$$X = \begin{bmatrix} i_{sd} & i_{sq} & i_{rd} & i_{rq} \end{bmatrix}^T$$

The state model can then be written as :

$$\dot{X} = A\,X + B\,U$$

With :

$$\dot{X} = \begin{bmatrix} \dfrac{d}{dt}i_{sd} & \dfrac{d}{dt}i_{sq} & \dfrac{d}{dt}i_{rd} & \dfrac{d}{dt}i_{rq} \end{bmatrix}^T$$

$$U = \begin{bmatrix} V_{sd} & V_{sq} & V_{rd} & V_{rq} \end{bmatrix}^T$$

$$A = \begin{bmatrix} -a_1 & a\omega + \omega_s & a_3 & a_5\omega \\ -a\omega - \omega_s & -a_1 & -a_5\omega & a_3 \\ a_4 & -a_6\omega & -a_2 & -\dfrac{\omega}{\sigma}+\omega_s \\ a_6\omega & a_4 & \dfrac{\omega}{\sigma}-\omega_s & -a_2 \end{bmatrix}, \quad B = \begin{bmatrix} b_1 & 0 & -b_3 & 0 \\ 0 & b_1 & 0 & -b_3 \\ -b_3 & 0 & b_2 & 0 \\ 0 & -b_3 & 0 & b_2 \end{bmatrix}$$

Where:

$$a = \frac{1-\sigma}{\sigma}, \quad a_1 = \frac{R_s}{\sigma L_s}, \quad a_2 = \frac{R_r}{\sigma L_r}, \quad a_3 = \frac{R_r M}{\sigma L_s L_r}, \quad a_4 = \frac{R_s M}{\sigma L_s L_r}, \quad a_5 = \frac{M}{\sigma L_s}, \quad a_6 = \frac{M}{\sigma L_r},$$

$$b_1 = \frac{1}{\sigma L_s}, b_2 = \frac{1}{\sigma L_r}, \quad b_3 = \frac{M}{\sigma L_s L_r}, \quad \sigma = 1 - \frac{M^2}{L_s L_r}$$

5. Field Oriented Control of DFIG:

In this section, the DFIM model can be described by the following state equations in the synchronous reference frame whose axis d is aligned with the stator flux vector, ($\phi_{sd} = \phi_s$ and $\phi_{sq} = 0$).

The control of the DFIG must allow a control independent of the active and reactive powers by the rotor voltages generated by an inverter.

By neglecting resistances of the stator phases the stator voltage will be expressed by:

$$V_{ds} = 0 \text{ and } V_{qs} = V_s \approx \omega_s \phi_s \tag{11}$$

We lead to an uncoupled power control; where, the transversal component i_{rq} of the rotor current controls the active power. The reactive power is imposed by the direct component i_{rd} .

$$P_s = -V_s \frac{M}{L_s} i_{rq} \tag{12}$$

$$Q_s = \frac{V_s^2}{\omega_s L_s} - V_s \frac{M}{L_s} i_{rd} \tag{13}$$

The arrangement of the equations gives the expressions of the voltages according to the rotor currents:

$$i_{rd} = -\frac{1}{\sigma T_r} i_{rd} + g\omega_s i_{rq} + \frac{1}{\sigma L_r} V_{rd} \tag{14}$$

$$i_{rq} = -\frac{1}{\sigma}\left(\frac{1}{T_r} + \frac{M^2}{L_S T_s . L_r}\right) i_{rq} - g\omega_s i_{rd} + \frac{1}{\sigma L_r} V_{rq} \tag{15}$$

With:

$$T_r = \frac{L_r}{R_r} \; ; \; T_s = \frac{L_s}{R_s} \; ; \sigma = 1 - \frac{M^2}{L_s . L_r}$$

Where:

i_{rd}, i_{rq} are rotor current components, ϕ_{sd}, ϕ_{sq} are stator flux components, V_{sd}, V_{sq} are stator voltage components, V_{rd}, V_{rq} rotor voltage components. R_s and R_r are stator and rotor resistances, L_s and L_s are stator and rotor inductances, M is mutual inductance, σ is leakage factor and p is number of pole pairs. C_e is the electromagnetic torque, C_r is the load torque, J is the moment of inertia of the DFIM, Ω is mechanical speed, ω_s is the stator pulsation, ω is the rotor pulsation, f is the friction coefficient, T_s and T_r are statoric and rotoric time-constant.

The inverter connected to the rotor of the DFIG must provide the necessary complement frequency in order to maintain constant the stator frequency despite the variation of the mechanical speed.

The system studied in the present paper is constituted of a DFIG directly connected through the stator windings to the network, and supplied through the rotor by a static frequency converter as presented in figure 3.

6. Sliding Mode Control:

A Sliding Mode Controller (SMC) is a Variable Structure Controller (VSC). Basically, a VSC includes several different continuous functions that can map plant state to a control surface, whereas switching among different functions is determined by plant state represented by a switching function (Nasri, A., 2008).
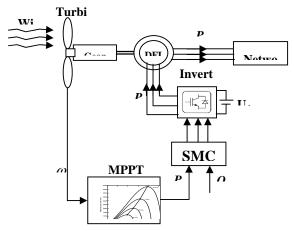

Fig. 3: DFIG variable speed wind energy conversion MPPT control.

The design of the control system will be demonstrated for a following nonlinear system (Youcef Bekakra, 2010):

$$\dot{x} = f(x,t) + B(x,t).u(x,t) \tag{16}$$

Where $x \in \square^n$ is the state vector, $u \in \square^m$ is the control vector, $f(x,t) \in \square^n$, $B(x,t) \in \square^{n \times m}$.

From the system (16), it possible to define a set S of the state trajectories x such as:

$$S = \{x(t) \mid \sigma(x,t) = 0\} \tag{17}$$

Where:

$$\sigma(x,t)=\left[\sigma_1(x,t),\sigma_2(x,t),...,\sigma_m(x,t)\right]^T \tag{18}$$

and $\left[.\right]^T$ denotes the transposed vector, S is called the sliding surface.

To bring the state variable to the sliding surfaces, the following two conditions have to be satisfied:

$$\sigma(x,t)=0, \quad \dot{\sigma}(x,t)=0 \tag{19}$$

The control law satisfies the precedent conditions is presented in the following form:

$$u = u^{eq} + u^{n} \tag{20}$$
$$u^{n} = -k_f\, sgn(\sigma(x,t))$$

Where u is the control vector, u^{eq} is the equivalent control vector, u^{n} is the switching part of the control (the correction factor), k_f is the controller gain. u^{eq} can be obtained by considering the condition for the sliding regimen, $\dot{\sigma}(x,t)=0$. The equivalent control keeps the state variable on sliding surface, once they reach it.

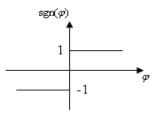For a defined function φ (Abid, M., 2008; Lo, J., Y. Kuo, 1998), (see figure 4):

Fig. 4: Sgn function.

$$sgn(\varphi)=\begin{cases} 1, & if \;\; \varphi>0 \\ 0, & if \;\; \varphi=0 \\ -1, & if \;\; \varphi>0 \end{cases} \tag{21}$$

The controller described by the equation (20) presents high robustness, insensitive to parameter fluctuations and disturbances, but it will have high-frequency switching (chattering phenomena) near the sliding surface due to sgn function involved. These drastic changes of input can be avoided by introducing a boundary layer with width ε (Youcef Bekakra, 2010). Thus replacing $sgn(\sigma(t))$ by $sat(\sigma(t)/\varepsilon)$ (saturation function), (see figure 5) in (20), we have:

$$u = u^{eq} - k_f\, sat(\sigma(x,t)) \tag{22}$$

Where $\varepsilon > 0$:

$$sat(\varphi)=\begin{cases} sgn(\varphi), & if \;\; |\varphi|\geq 1 \\ \varphi, & if \;\; |\varphi|<1 \end{cases} \tag{23}$$
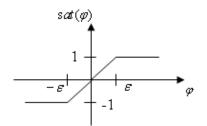
Fig. 5: Saturation (*sat*) function.

Consider a Lyapunov function (Abid, M., 2008):

$$V = \frac{1}{2}\sigma^2 \tag{24}$$

From Lyapunov theorem we know that if $\dot{V}$ is negative definite, the system trajectory will be driven and attracted toward the sliding surface and remain sliding on it until the origin is reached asymptotically (Youcef Bekakra, 2010):

$$\dot{V} = \frac{1}{2}\frac{d}{dt}\sigma^2 = \sigma\,\dot{\sigma} \leq -\eta|\sigma| \tag{25}$$

Where η is a strictly positive constant.
In this paper, we use the sliding surface proposed par J.J. Slotine,

$$\sigma(x,t) = \left(\frac{d}{dt}+\lambda\right)^{n-1} e \tag{26}$$

Where:

$x = [x,\dot{x},...,x^{n-1}]^T$ is the state vector, $x^d = [x^d,\dot{x}^d,...,x^d]^T$ is the desired state vector, $e = x^d - x = \left[e,\dot{e},...,e^{n-1}\right]$ is the error vector, and λ is a positive coefficient, and n is the system order.

Commonly, in DFIM control using sliding mode theory, the surfaces are chosen as functions of the error between the reference input signal and the measured signals (Youcef Bekakra, 2010).

7. Application of Sliding Mode Control to DFIG:

The rotor currents (which are linked to active and reactive powers by equations (12) and (13), quadrature rotor current i_{rq} linked to active power P_s and direct rotor current i_{rd} linked to reactive power Q_s) have to track appropriate current references, so, a sliding mode control based on the above Park reference frame is used.

7.1. Quadrature Rotor Current Control with SMC:

The sliding surface representing the error between the measured and reference quadrature rotor current is given by this relation:

$$e = i_{rq}^* - i_{rq} \tag{27}$$

For $n = 1$, the speed control manifold equation can be obtained from equation (26) as follow:

$$\sigma(i_{rq}) = e = i_{rq}^* - i_{rq} \tag{28}$$

$$\dot{\sigma}(i_{rq}) = \dot{i}_{rq}^* - \dot{i}_{rq} \tag{29}$$

Substituting the expression of $\dot{i}_{rq}$ equation (15) in equation (29), we obtain:

$$\sigma(\dot{i}_{rq}) = \dot{i}_{rq}^{\,*} - \left(-\frac{1}{\sigma}\left(\frac{1}{T_r} + \frac{M^2}{L_S T_s L_r}\right) i_{rq} - g\,\omega_s i_{rd} + \frac{1}{\sigma L_r} V_{rq} \right) \tag{30}$$

We take :

$$V_{rq} = V_{rq}^{\,eq} + V_{rq}^{\,n} \tag{31}$$

During the sliding mode and in permanent regime, we have:

$$\sigma(i_{rq}) = 0,\ \dot{\sigma}(i_{rq}) = 0, V_{rq}^{\,n} = 0$$

Where the equivalent control is:

$$V_{rq}^{\,eq} = \left(\dot{i}_{rq}^{\,*} + \frac{1}{\sigma}\left(\frac{1}{T_r} + \frac{M^2}{L_S T_s L_r}\right) i_{rq} + g\,\omega_s i_{rd} \right) \sigma L_r \tag{32}$$

Therefore, the correction factor is given by :

$$V_{rq}^{\,n} = k_{V_{rq}} sat\left(\sigma(i_{rq})\right) \tag{33}$$

$k_{V_{rq}}$: positive constant.

7.2. Direct Rotor Current Control with SMC:
The sliding surface representing the error between the measured and reference direct rotor current is given by this relation:

$$e = i_{rd}^{\,*} - i_{rd} \tag{34}$$

For $n = 1$, the speed control manifold equation can be obtained from equation (26) as follow:

$$\sigma(i_{rd}) = e = i_{rd}^{\,*} - i_{rd} \tag{35}$$

$$\dot{\sigma}(i_{rd}) = \dot{i}_{rd}^{\,*} - \dot{i}_{rd} \tag{36}$$

Substituting the expression of $\dot{i}_{rd}$ equation (14) in equation (36), we obtain:

$$\dot{\sigma}(i_{rd}) = \dot{i}_{rd}^{\,*} - \left(-\frac{1}{\sigma T_r} i_{rd} + g\,\omega_s i_{rq} + \frac{1}{\sigma L_r} V_{rd} \right) \tag{37}$$

We take:

$$V_{rd} = V_{rd}^{\,eq} + V_{rd}^{\,n} \tag{38}$$

During the sliding mode and in permanent regime, we have:

$$\sigma(i_{rd}) = 0,\ \dot{\sigma}(i_{rd}) = 0, V_{rd}^{\,n} = 0$$

Where the equivalent control is:

$$V_{rd}^{\,eq} = \left(\dot{i}_{rd}^{\,*} + \frac{1}{\sigma T_r} i_{rd} - g\,\omega_s i_{rq} \right) \sigma L_r \tag{39}$$

Therefore, the correction factor is given by:

$$V_{rd}^{n} = k_{V_{rd}} sat\left(\sigma(i_{rd})\right) \tag{40}$$

$k_{V_{rd}}$: positive constant.

8. Simulation Results:

The wind energy conversion system is simulated using MATLAB software.

The DFIG used in this work is a 4 kW, whose nominal parameters are indicated in the following:

Rated values: 4 kW , 220/380 V, 15/8.6 A.

Rated parameters: $R_s = 1.2\ \Omega$, $R_r = 1.8\ \Omega$, $L_s = 0.1554\ H$, $L_r = 0.1568\ H$, $M = 0.15\ H$, $p = 2$.

Wind turbine parameters are: R (Blade length) $= 3\ m$, $\rho = 1.22\ Kg/m^3$, G (Gearbox) $= 5.4$, Nombre of blades $= 3$

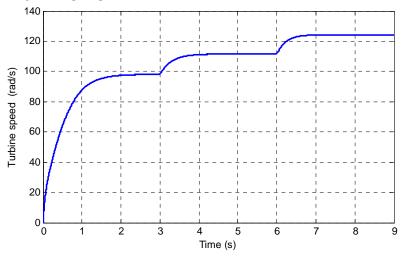**Fig. 6:** A step change wind speed profiles.

Fig. 7: Speed turbine according the MPPT.

In order to evaluate the MPPT control strategy proposed in this paper, MATLAB is used to carry out the simulation. We proposed a step change in wind speed is simulated in figure 6, the wind speed is start at 5 m per second , at 3 second, the wind speed suddenly become 6 m per second , as 6 second, the wind speed is 7 m per second.

The figure 7 presents the turbine speed. Figures 8 presents the stator active power and its reference profiles (with its zoom) resulting of the MPPT and injected into the grid. Figures 9 shows the stator reactive power and its reference profiles (with its zoom) versus time. Figures 10 and 11 present respectively stator and rotor. Figure 12 presents the power coefficient.
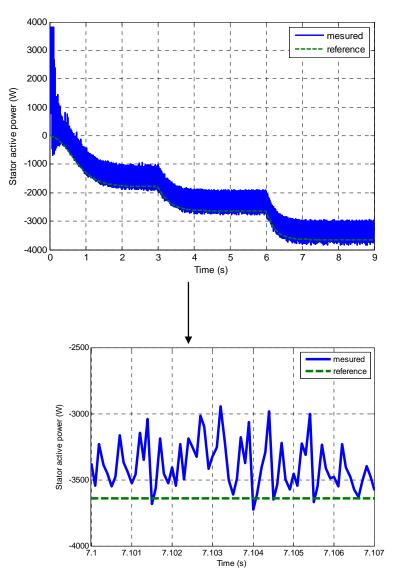
Fig. 8: Stator active power injected in the grid according the MPPT and its zoom.

As can be seen from the plots, the stator active power is controlled according to the MPPT strategy, and to guarantee a unity power factor at the stator side, the reactive power is maintained to zero.

The power coefficient is kept around its optimum (see figure 12).

The figure 13 presents wind turbine output power characteristics with MPPT process. For a variable wind figure 13 shows an operation with optimum capacity. We note oscillations around the optimal points as in figure 2.

9. Conclusion:

In this paper a variable structure control based on a sliding mode control (SMC) of a doubly fed induction generator (DFIG) grid-connected wind energy conversion system, incorporating a maximum power point tracker (MPPT) for dynamic power control has been presented. This structure has been used for reference tracking of active and reactive powers exchanged between the stator and the grid by controlling the rotor converter. Simulation results show good decoupling between stator active and reactive power and good performance obtained in the presence of the variations of wind speed. The obtained results demonstrate that the proposed DFIG system control operating at the variable speed may be considered as an interesting way for problems solution in renewable energy area.
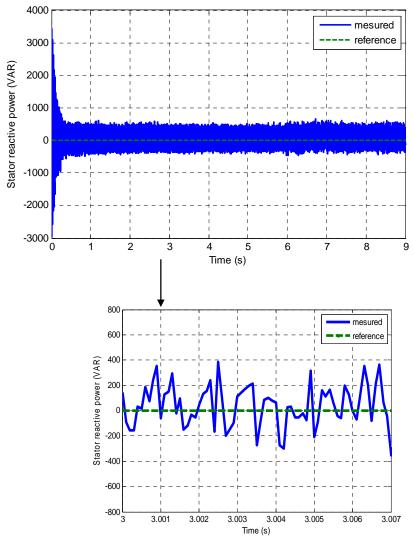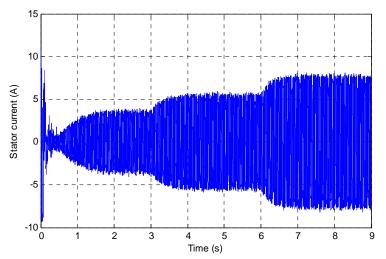
Fig. 9: Stator reactive power and its zoom.
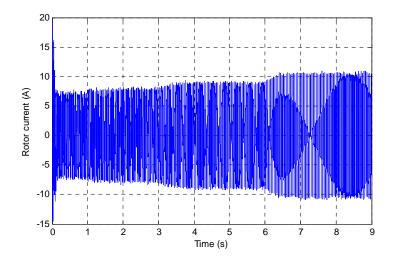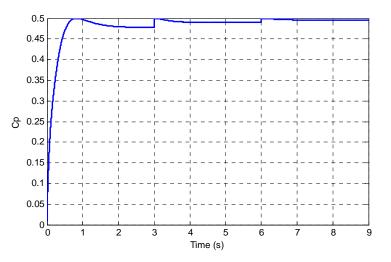

Fig. 10: Stator current.

Fig. 11: Rotor current.

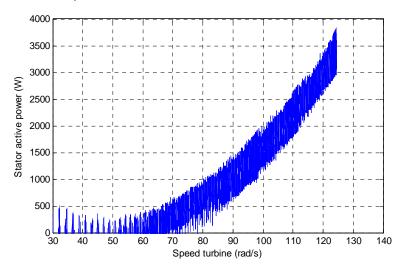**Fig. 12:** Power Coefficient C_p variation.

Fig. 13: Stator active power versus speed turbine.

REFERENCES

Abid, M., A. Mansouri, A. Aissaoui, B. Belabbes, 2008. "Sliding mode application in position control of an induction machine," Journal of electrical engineering, 59(6): 322-327.

Ali M. Eltamaly, A.I. Alolah, Mansour H. Abdel-Rahman, 2010. ''Modified DFIG Control Strategy for Wind Energy Applications," SPEEDAM 2010, International Symposium on Power Electronics, Electrical Drives, Automation and Motion, 978-1-4244-4987-3/10/$25.00 ©2010 IEEE, pp: 659-653.

Guo-qing, W.U., N.I. Hong-jun, W.U. Guo-xiang, Z.H.O.U. Jing-ling, Zhu Wei-nan, M.A.O. Jing-feng, C.A.O. Yang, 2010. ''On maximum power point tracking control strategy for variable speed constant frequency wind power generation ," Journal of Chongqing University (English Edition) [ISSN 1671-8224], [ISSN 1671-8224], 9(1): 21-28.

Hazzab, A., I.K. Bousserhane, M. Kamli, M. Rahli, 2005. "Adaptive Fuzzy PI-Sliding Mode Controller for Induction Motor Speed Control," International Journal of Emerging Electric Power Systems, 4(1): Article 1084: 1-13.

Jeong-Ik Jang, Young-Sin Kim, Dong-Choon Lee, 2006. ''Active and Reactive Power Control of DFIG for Wind Energy Conversion under Unbalanced Grid Voltage,'' IPEMC, 1-4244-0449-5/06/$20.00 ©2006 IEEE.

Lo, J., Y. Kuo, 1998. "Decoupled fuzzy sliding mode control," IEEE Trans. Fuzzy Syst., 6(3): 426-435.

Nasri, A., A. Hazzab, I.K. Bousserhane, S. Hadjiri, P. Sicard, 2008. Two wheel speed robust sliding mode control for electrical vehicle drive, Serbian Journal of Electrical Engineering, 5(2): 199-216.

Salma El-Aimani, 2004. ''Modélisation de différentes technologies d'éoliennes intégrées dans un réseau de moyenne tension,'' Thèse de doctorat, Université des Sciences et technologies de Lille.

Utkin, V.I., 1993. "Sliding mode control design principles and applications to electric drives," IEEE Trans. on Industrial Electronics, 40(1): 23-36.

Xuemei Zheng, Lin Li, Dianguo Xu, Jim Platts, 2009. ''Sliding Mode MPPT Control of Variable Speed Wind Power System,'' 978-1-4244-2487-0/09/$25.00 ©2009 IEEE, Power and Energy Engineering Conference, 2009. APPEEC 2009, pp : 1-4.

Youcef Bekakra, Djilani Ben Attous, 2010. ''Speed and Flux Control for DFOC of Doubly Fed Induction Machine using Sliding Mode Controller,'' Acta Electrotechnica et Informatica, 10(4): 75-81, ISSN 1335-8243.